Epithelial cell α3β1 integrin links β-catenin and Smad signaling to promote myofibroblast formation and pulmonary fibrosis

Kevin K. Kim,[1] Ying Wei,[1] Charles Szekeres,[2] Matthias C. Kugler,[1] Paul J. Wolters,[1]
Marla L. Hill,[1] James A. Frank,[3] Alexis N. Brumwell,[1] Sarah E. Wheeler,[1]
Jordan A. Kreidberg,[2] and Harold A. Chapman[1]

[1]Pulmonary and Critical Care Division, Department of Medicine, and Cardiovascular Research Institute, UCSF, San Francisco, California, USA.
[2]Children's Hospital and Harvard Medical School, Boston, Massachusetts, USA. [3]Pulmonary and Critical Care Division,
Department of Medicine, and San Francisco VA Medical Center, San Francisco, California, USA.

Pulmonary fibrosis, in particular idiopathic pulmonary fibrosis (IPF), results from aberrant wound healing and scarification. One population of fibroblasts involved in the fibrotic process is thought to originate from lung epithelial cells via epithelial-mesenchymal transition (EMT). Indeed, alveolar epithelial cells (AECs) undergo EMT in vivo during experimental fibrosis and ex vivo in response to TGF-β1. As the ECM critically regulates AEC responses to TGF-β1, we explored the role of the prominent epithelial integrin α3β1 in experimental fibrosis by generating mice with lung epithelial cell–specific loss of α3 integrin expression. These mice had a normal acute response to bleomycin injury, but they exhibited markedly decreased accumulation of lung myofibroblasts and type I collagen and did not progress to fibrosis. Signaling through β-catenin has been implicated in EMT; we found that in primary AECs, α3 integrin was required for β-catenin phosphorylation at tyrosine residue 654 (Y654), formation of the pY654–β-catenin/pSmad2 complex, and initiation of EMT, both in vitro and in vivo during the fibrotic phase following bleomycin injury. Finally, analysis of lung tissue from IPF patients revealed the presence of pY654–β-catenin/pSmad2 complexes and showed accumulation of pY654–β-catenin in myofibroblasts. These findings demonstrate epithelial integrin–dependent profibrotic crosstalk between β-catenin and Smad signaling and support the hypothesis that EMT is an important contributor to pathologic fibrosis.

Introduction

Progressive fibrosis of the lung, especially that of idiopathic pulmonary fibrosis (IPF), is thought to be a consequence of aberrant wound healing resulting in progressive scarification (1, 2). Fibroblast expansion and activation leading to collagen fibril deposition is considered to be a final common pathway, and hence much attention has been directed at mechanisms that lead to fibroblast proliferation and synthesis of matrix proteins. In addition to expansion/activation of resident fibroblasts, fibrogenic fibroblasts may also originate from lung epithelial cells through epithelial-mesenchymal transition (EMT) (3–6). In this scenario, injurious stimuli lead to activation of certain key mediators, which cause some epithelial cells to become reprogrammed as fibroblasts. While EMT in the lung is not mutually exclusive of endogenous fibroblast activation, these processes are likely regulated very differently.

EMT is a process involving loss of apical-basal polarity, loss of cell-cell contacts, detachment from the basement membrane, cytoskeletal rearrangement, and migration into the provisional matrix. These vast phenotypic changes are accompanied by significant changes in molecular expression within the cell, requiring extensive coordination (7). We recently reported that alveolar epithelial cells (AECs) undergo EMT in vivo in an animal model of pulmonary fibrosis by using a murine system in which AECs are genetically tagged to specifically and permanently express a reporter protein (8). We further demonstrated that AECs undergo EMT ex vivo via activation of endogenous TGF-β1.

TGF-β1 signaling has been implicated in many models of EMT and fibrosis (9–11). TGF-β1 signaling can be regulated at multiple levels from production and activation of TGF-β1 to formation of a Smad transcriptional complex with various Smad co-regulators (12, 13). Importantly, TGF-β1 signaling is not an on/off response, rather cells can respond in a variety of different ways to active TGF-β1 depending on convergence with other signaling pathways. In primary AECs the ECM is an important determinant to the cellular response to TGF-β1, with provisional matrix proteins such as fibronectin (Fn) driving EMT and basement membrane proteins such as laminin and type IV collagen preventing EMT (8). The mechanisms by which the ECM regulates EMT and fibrosis remain to be elucidated but likely involve signaling through integrin receptors.

Integrins are transmembrane adhesion molecules which bind to specific ECM ligands. Integrin activation can initiate intracellular signaling or influence signaling through other receptors (14, 15). For example, β1 integrins have been shown to regulate signaling through transmembrane growth factor receptors such as the epidermal growth factor receptor and the platelet-derived growth factor receptor (16, 17). One report, using a β1 integrin blocking antibody, demonstrated that β1 integrins are critical for TGF-β1–mediated transcription and epithelial cell plasticity in vitro (18).
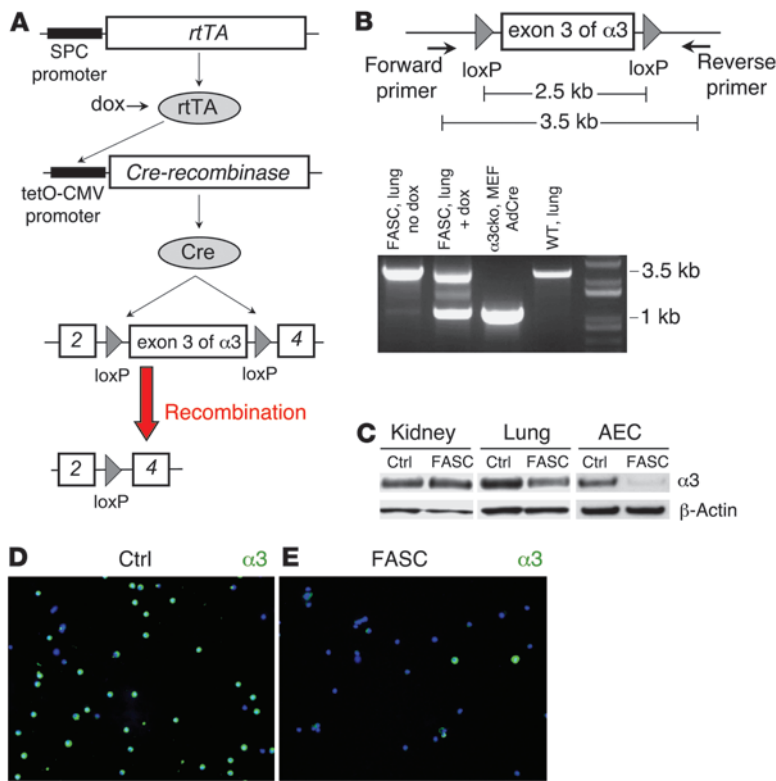
Figure 1
Lung epithelial cell–specific loss of α3 integrin in FASC mice. (**A**) In triple transgenic FASC mice, rtTA is expressed in lung epithelial cells using the human SPC promoter. In the presence of doxycycline (dox), rtTA is an active transcriptional factor leading to expression of Cre recombinase and removal of the floxed exon 3 of the α3 integrin gene, resulting in lung epithelial cell–specific loss of α3 integrin. (**B**) PCR using primers that encompass the floxed region of the floxed α3 integrin gene. DNA from lungs of FASC mice fed doxycycline revealed a 1-kb band consistent with the recombined floxed α3 integrin and a 3.5-kb band corresponding to non-recombined floxed α3 integrin in non-epithelial cells of the lung. Littermate control mice and FASC mice not on doxycycline only demonstrated the 3.5-kb band. Murine embryonic fibroblasts (MEFs) derived from a floxed α3 integrin (α3cko) mouse and treated in vitro with adenovirus expressing Cre (AdCre) was used as a positive control and only exhibited the 1-kb band. (**C**) Immunoblot demonstrating normal levels of α3 integrin in kidney lysate of a FASC mouse compared with littermate controls (Ctrl) lacking 1 of the transgenes but an approximately 50% reduction of α3 integrin in whole lung lysate and an approximately 80% reduction of α3 integrin in lysates of isolated AECs. (**D** and **E**) Immunostaining of isolated AECs demonstrates that about 60%–90% of FASC AECs (**E**) lack expression of α3 integrin compared with littermate control AECs (**D**).

α3β1 integrin is a laminin receptor that also localizes to sites of cell-cell contacts through its interaction with the E-cadherin/β-catenin complex (19). Signaling through β-catenin has been implicated in both EMT and pulmonary fibrosis (20), though this is largely thought to involve the Wnt pathway of stabilization of β-catenin. Thus, an intriguing hypothesis is that α3β1 integrin is a key regulator of AEC EMT through its ability to coordinate phenotypic changes involving cell-cell and cell-matrix interactions with transcriptional reprogramming.

To explore the function of α3 integrin in EMT and pulmonary fibrosis, we used triple transgenic mice with lung epithelial cell–specific loss of α3 integrin. These mice had a normal acute response to bleomycin injury but failed to progress to fibrosis and had markedly impaired EMT. These studies also revealed α3β1 integrin as a critical coordinator of prominent EMT signaling pathways involving β-catenin and pSmad2.

Results

Generation of floxed α3 integrin/SPC-rtTA/tetO-cre mice (lung epithelial cell–specific loss of α3 integrin). To explore the in vivo significance of AEC α3 integrin, we used the cre-lox system, in which tissue-specific expression of cre-recombinase results in permanent removal of sequences of DNA flanked by loxP sites (floxed) within those tissues. We generated triple transgenic mice by crossing *floxed α3 integrin* mice with mice carrying the *human SPC promoter-rtTA* and *tetO-CMV-Cre* transgenes (8) (Figure 1A). Hereafter, these mice will be referred to as "floxed α3 integrin/SPC-rtTA/tetO-cre" (FASC). Lung epithelial cell–specific recombination was verified by several techniques. PCR primers encompassing the floxed region were designed. DNA from lungs of FASC mice fed doxycycline revealed a 1-kb band consistent with the recombined floxed α3 integrin and

a 3.5-kb band corresponding to non-recombined floxed α3 integrin in nonepithelial cells of the lung. Littermate control mice and FASC mice not on doxycycline only demonstrated the 3.5-kb band (Figure 1B). FASC mice had normal levels of α3 integrin in kidney lysate compared with littermate controls lacking one of the transgenes but an approximately 50% reduction of α3 integrin in whole lung lysate and an approximately 80% reduction of α3 integrin in lysates of isolated AECs (Figure 1C). Staining of isolated AECs revealed that approximately 60%–90% of FASC AECs lacked expression of α3 integrin (Figure 1, D and E). Collectively, these data confirm lung epithelial cell–specific loss of α3 integrin in FASC mice.

FASC mice have a normal acute lung injury response to bleomycin injury. In contrast to α3 integrin–null mice, which die perinatally due to renal failure (21), FASC mice have a normal lifespan and body weight compared with their WT littermates. Alveolar architecture was grossly preserved (Figure 2, A and B), and there were no differences in total lung capacity and airway resistance (data not shown). Interestingly, FASC mice demonstrated a mild type II AEC hyperplasia demonstrated by increased numbers of pro-surfactant protein C–positive (pro-SPC–positive) cells (Figure 2, C and D) and increased numbers of Ki67-positive cells (0.89% vs. 0.41%) from immunofluorescence staining of lung sections (Supplemental Figure 1; supplemental material available online with this article; doi:10.1172/JCI36940). This approximately 2-fold increase in type II AECs was not progressive but was maintained over the lifespan of the mouse. As expected, an increase in pro-SPC was confirmed by immunoblot of whole lung lysates of FASC mice (Figure 2G).

Surprisingly, FASC lung sections stained by trichrome revealed increased collagen staining diffusely within the alveolar septa with otherwise preserved architecture compared with littermate control mice (Figure 2, E and F). The appearance of alveolar wall collagen
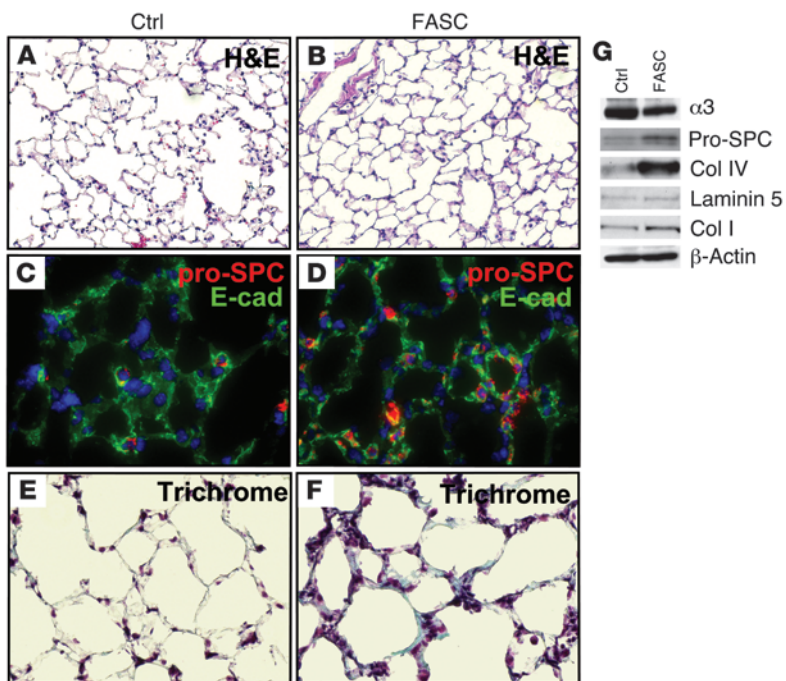
Figure 2
Baseline phenotypes of FASC lungs. Littermate control (**A**, **C**, and **E**) and FASC (**B**, **D**, and **F**) lung sections. (**A** and **B**) Lung sections (original magnification, ×20) stained by H&E demonstrated similar alveolar architecture. (**C** and **D**) Lung sections (original magnification, ×60) immunostained for E-cadherin (E-cad, green) and pro-SPC (red) demonstrated a similar E-cadherin staining pattern and increased numbers of pro-SPC–positive cells in FASC lungs. (**E** and **F**) Lung sections (original magnification, ×60) stained with trichrome demonstrated increased diffuse staining within the alveolar basement membranes of FASC mice. (**G**) Immunoblot showed decreased expression of α3 integrin, increased expression of pro-SPC, a clear increase in collagen IV (col IV), similar levels of laminin 5, and a slight increase in collagen I (col I) in FASC lung lysate compared with littermate control lung lysate.

was not strictly a developmental abnormality because FASC mice started on doxycycline postnatally also displayed increased collagen after several weeks (data not shown). While apparent from tissue staining, the degree of collagen deposition did not result in significant differences in baseline compliance between normal and FASC mice (Figure 3E) and did not have an impact on lifespan. Because trichrome staining does not distinguish among different collagen subtypes, we analyzed FASC and control mouse lungs for type IV collagen, a normal major component of the alveolar basement membrane, and type I collagen, prominent in pulmonary fibrosis. Indeed, FASC mice demonstrated a clear increase in type IV collagen by immunoblotting and immunostaining consistent with the increased trichrome staining. Levels of type I collagen and laminin 5, the main α3β1 integrin ECM ligand, were similar between FASC and littermate control mice (Figure 2G).

FASC mice also exhibited increased BAL cellularity both at baseline and 5 days after bleomycin injury compared with littermate controls that was apparent in lung sections (Figure 3, A and B) and by BAL cell counts. BAL cell differential was similar between FASC and littermate control mice, both at baseline and after bleomycin injury (data not shown). Importantly, FASC lungs demonstrated normal staining for E-cadherin (Figure 2, C and D) and no differences in lung permeability at rest or acutely after bleomycin injury as measured by I^{125}-albumin uptake in the lungs, BAL total protein, and excess lung water, all reflecting a normal vascular response to injury and intact epithelial barrier function (Figure 3). Despite this normal permeability response, FASC mice trended toward lower compliance acutely after bleomycin injury ($P = 0.09$), likely due to the exaggerated inflammation (Figure 3E).

α3 integrin is critical for pulmonary fibrosis. Bleomycin injury can initiate lung fibrosis in addition to acute lung injury, and recent evidence suggests that these pathways are distinct (22, 23). To explore the role of α3 integrin in pulmonary fibrosis, 6-week-old FASC mice or littermate controls were injected intratracheally with saline or bleomycin. We first looked at the accumulation of

myofibroblasts, which are thought to be important fibrogenic effector cells (24). As expected, control mice developed robust myofibroblast accumulation 17 days after bleomycin injury, as indicated by staining lung sections for α-SMA. In contrast, FASC mice demonstrated a minimal increase in the number of myofibroblasts compared with saline-treated mice (Figure 4, A–C). Three weeks after bleomycin injury, the extent of fibrosis was determined by several methods. Lung fibrosis is characterized by the accumulation of fibrillar collagens, such as type I collagen. Immunostaining for collagen I demonstrated thick bands of fibrosis in control mice, while FASC mice were almost completely protected from bleomycin-induced fibrosis (Figure 4, D and E). Collagen I content, quantified by immunoblot from whole lung lysates, showed no significant increase after bleomycin injury in FASC mice (Figure 4, F and H). Lung collagen content was further assessed by hydroxyproline content (Figure 4G). Saline-treated FASC mice demonstrated a 2-fold increase in hydroxyproline compared with saline-treated littermate control mice, consistent with the increased levels of type IV collagen in FASC mice. Completely uninjured FASC mice exhibited a similar increase in hydroxyproline, suggesting that this increase in hydroxyproline was not due to a response to saline injection (data not shown). Again, FASC mice demonstrated a blunted response to bleomycin with no significant increase in hydroxyproline after bleomycin injury compared with a 2-fold increase in injured control mice. Six-month-old FASC and control mice assessed by hydroxyproline had a similar pattern, with saline-treated FASC mice having an approximately 3-fold increase in hydroxyproline compared with control mice at baseline and a blunted increase in hydroxyproline after bleomycin injury (Supplemental Figure 2).

α3 integrin regulates EMT in vivo. Because loss of α3 integrin in FASC mice is limited to lung epithelial cells, we hypothesized that protection from myofibroblast accumulation and fibrosis could be due to ineffective EMT. EMT has been reported in several models of tissue fibrosis (8, 25, 26), but has not yet been demonstrated
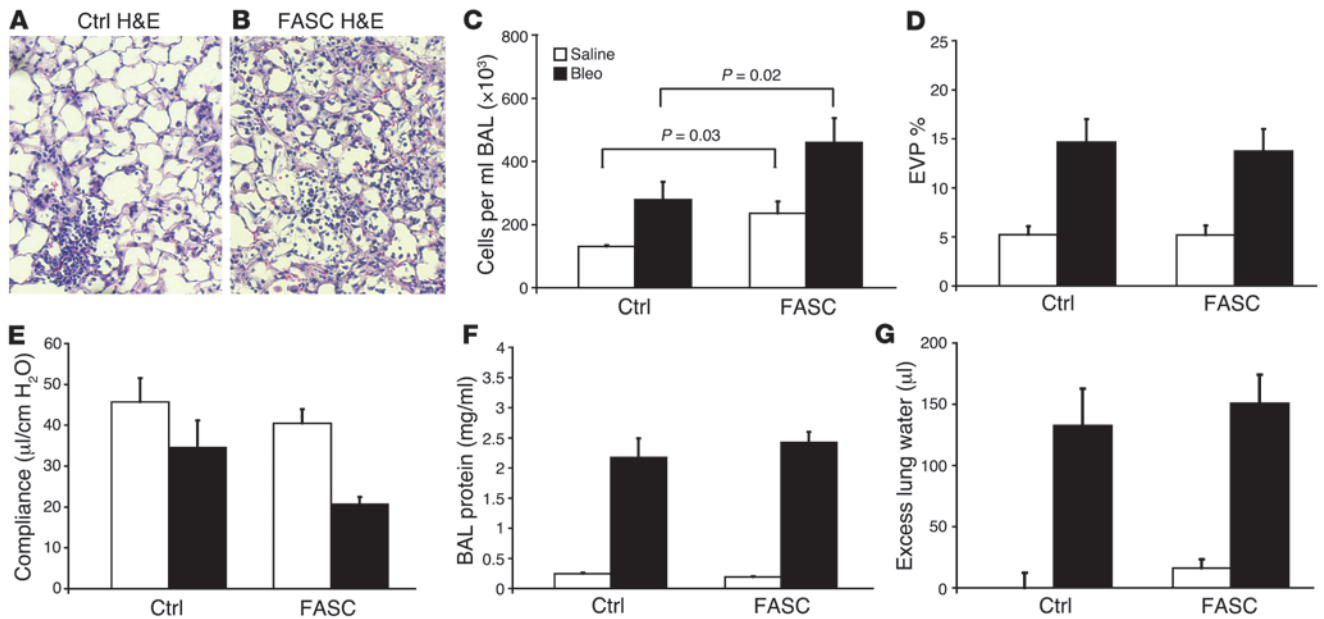
Figure 3
Preserved acute lung injury response in FASC mice. (**A** and **B**) Five days after intratracheal bleomycin injury, littermate control (**A**) and FASC (**B**) lung sections (original magnification, ×20) were stained with H&E and demonstrated increased inflammation in FASC mice. (**C**) Cell counts from BAL of littermate control and FASC mice 5 days after intratracheal saline or bleomycin injury. FASC mice had an increased number of cells compared with littermate controls ($n = 4–6$ per group). (**D**) Lung permeability determined by extravasation of intravascular ^{125}I-albumin into the lungs and expressed as EVP%. FASC and littermate control mice demonstrated similar permeability 5 days after bleomycin injury ($n = 4$ per group). (**E**) Lung compliance (μl/cm H_2O) was determined from anesthetized and paralyzed ventilated mice. FASC and littermate control mice demonstrated a decrease in compliance 5 days after bleomycin injury. There was a trend toward less compliance in FASC mice after bleomycin injury compared with littermate control mice after bleomycin injury ($P = 0.09$; $n = 4$ per group). (**F**) Total protein concentration (mg/ml) from BAL 5 days after intratracheal saline or bleomycin injury. FASC and littermate control mice demonstrated a similar increase in BAL protein after bleomycin injury ($n = 4–6$ per group). (**G**) Excess lung water (determined as described in Methods) increased similarly in FASC and littermate control mice 5 days after bleomycin injury ($n = 4$ per group).

in the bleomycin model of lung fibrosis. To determine whether α3 integrin regulates EMT in vivo, we first assessed whether EMT occurs in this model. We developed triple transgenic reporter mice containing at least 1 copy of the human *SPC-rtTA*, *tetO-CMV-Cre*, and *ZEG* (floxed lacZ, EGFP) (27) transgenes, resulting in genetically tagged lung epithelial cells that permanently express GFP. Mice were given doxycycline throughout gestation, and lung epithelial cell–specific expression of GFP was confirmed by several techniques. Frozen lung sections stained for GFP revealed robust GFP expression within lung epithelial cells, predominantly pro-SPC–positive AECs, while mesenchymal structures within the lung (smooth muscle layers within vessels and airways) were completely GFP negative (Supplemental Figure 3). Several extrapulmonary organs were examined by immunostaining and immunoblot and revealed no expression of GFP. Primary AECs isolated from triple transgenic mice and littermate control mice were analyzed by flow cytometry, demonstrating that approximately 10%–40% of isolated type II AEC were GFP positive. Thus, GFP expression is specific for lung epithelial cells, but with a low recombination efficiency in *ZEG/SPC-rtTA/tetO-CMV-Cre* mice. Littermate control mice lacking either the *SPC-rtTA* or the *tetO-CMV-Cre* transgenes revealed no expression of GFP by these techniques (data not shown).

EMT during fibrogenesis was observed in the bleomycin model using these reporter mice by several methods. Triple transgenic mice were treated with bleomycin or saline, then analyzed after

17 days. Whole lung, single-cell suspensions were prepared and sorted for GFP-positive cells. As expected, cells from littermate control mice lacking any one of the transgenes did not express GFP even after bleomycin injury (Figure 5, B and C). Epithelial cell–derived, GFP-positive cells from triple transgenic reporter mice given saline or bleomycin were analyzed by immunoblot (Figure 5D) and immunostain for mesenchymal markers (Figure 5, E–G). Immunoblot revealed marked de novo expression of α-SMA and loss of pro-SPC within GFP-positive cells from bleomycin-injured mice compared with saline-treated mice. By immunostain, GFP-positive cells from saline-treated mice revealed no staining for mesenchymal markers, while in the bleomycin-injured mice, a surprisingly high percentage of epithelium-derived cells expressed classic mesenchymal markers (α-SMA, vimentin, and procollagen I). Finally, lung sections from bleomycin-injured and saline-treated mice were stained for GFP and α-SMA. Again, numerous cells costaining for GFP and α-SMA were identified in bleomycin-injured mice, but none in saline-treated mice (Figure 6, A and B). These EMT-derived cells were found within the interstitium and were not observed on the surface of the epithelial lumen.

To study the function of AEC α3 integrin in fibrosis, we established quadruple transgenic mice. Saline or bleomycin was intratracheally injected into *ZEG/SPC-rtTA/tetO-Cre/α3$^{fl/fl}$* (ZEG-FASC) and littermate *ZEG/SPC-rtTA/tetO-Cre/α3$^{fl/WT}$* or *ZEG/SPC-rtTA/tetO-Cre/α3$^{WT/WT}$* (ZEG-control), and the EMT response was deter-
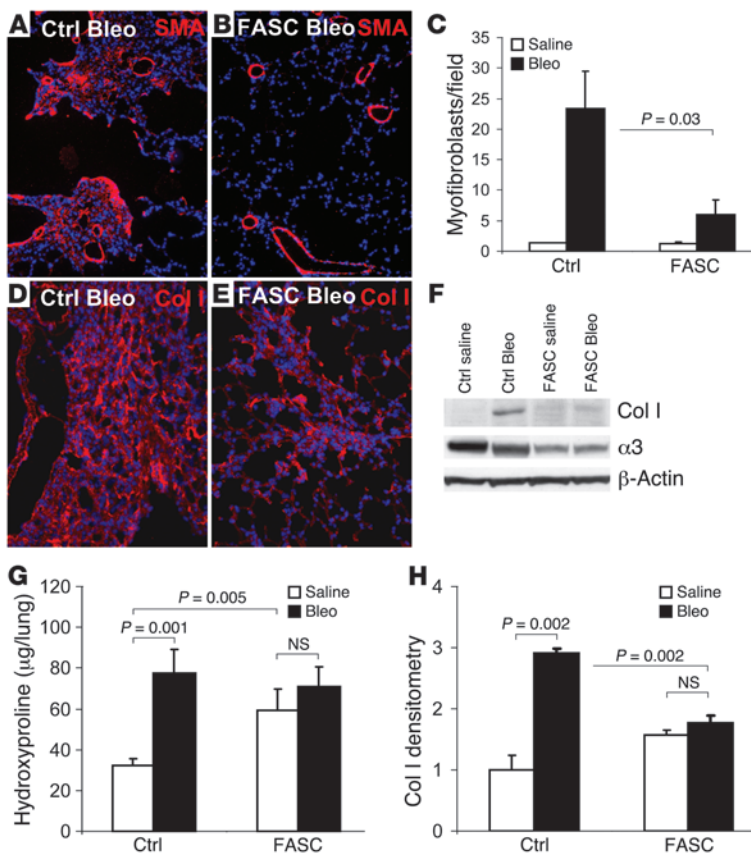
Figure 4
FASC mice have impaired myofibroblast accumulation and type I collagen response to bleomycin injury. (**A** and **B**) Lung sections (original magnification, ×20) from littermate control (**A**; Ctrl Bleo) and FASC (**B**; FASC Bleo) mice 17 days after intratracheal bleomycin injury immunostained for α-SMA. (**C**) Quantification of α-SMA–positive myofibroblasts revealed that FASC mice developed fewer α-SMA–positive myofibroblasts compared with controls. (**D** and **E**) Lung sections (original magnification, ×20) from littermate control mice lacking at least 1 of the 3 transgenes (**D**) and FASC mice (**E**) were stained for type I collagen 21 days after intratracheal injection with bleomycin. (**F**) Type I collagen content from whole lung lysate from littermate control and FASC mice 21 days after intratracheal injection with saline was analyzed by immunoblot. (**G**) Hydroxyproline assay from entire left lung of FASC or littermate control mice 21 days after intratracheal injection of saline or bleomycin. Uninjured FASC mice had increased levels of hydroxyproline and a blunted increase in hydroxyproline after bleomycin injury (*n* = 7–16 per group). (**H**) Relative densitometry of immunoblots for type I collagen from lung lysate of FASC or littermate control mice 21 days after intratracheal saline or bleomycin injection. FASC mice had significantly less type I collagen after bleomycin injury compared with control mice (*n* = 3 per group).

mined after 17 days by immunostaining lung sections (Figure 6). In saline-treated mice, GFP expression was confined to lung epithelial cells (data not shown). In ZEG-control mice injured with bleomycin (Figure 6, A and B), numerous GFP-positive cells also expressed α-SMA (7.0%; Figure 6C), indicating epithelial cell–derived myofibroblasts. In contrast, ZEG-FASC mice injured with bleomycin (data not shown) had much less EMT (1.4%; Figure 6C).

Overall, these findings indicate that lung epithelial cell α3β1 integrin is not required for normal lung epithelial cell barrier function but is required for patterned responses of the lung to at least one well-defined injurious stimulus, bleomycin. Although it is unlikely that all myofibroblasts are derived from epithelial cells, the data indicate that myofibroblast development occurs in an epithelial α3 integrin–dependent manner and that EMT-derived myofibroblasts clearly appear following bleomycin injury, accounting for a significant fraction of these myofibroblasts. Ineffective myofibroblast development in the absence of α3 integrin likely accounts for the greatly attenuated fibrotic response. We next considered a mechanism by which α3 integrin could regulate EMT and fibrogenesis.

α3 integrin is required for tyrosine phosphorylation of β-catenin and β-catenin/pSmad2 complex formation. We have previously shown that primary AECs cultured on provisional matrix proteins, such as Fn, undergo EMT via activation of endogenous TGF-β1 (8). Primary AECs from control and FASC mice were analyzed immediately after isolation and 4 days after culturing cells on Fn-coated plates. As expected, control AECs demonstrated a mesenchymal morphology (Figure 7A and Supplemental Figure 4A), upregulated classic mesenchymal markers α-SMA, collagen I, and vimentin, and

completely lost expression of pro-SPC (Figure 7C). FASC AECs maintained an epithelial morphology (Figure 7B and Supplemental Figure 4B) and had a dramatically limited EMT with weak upregulation of several mesenchymal markers even though pro-SPC expression was largely lost over time in culture.

FASC and control AECs had similar levels of Smad2 phosphorylation at day 4 after plating on Fn (Figure 7C) and at all other time points examined from day 2 to day 7 (data not shown), indicating that α3β1 integrin does not affect endogenous TGF-β1 production, activation, TGF-β1 receptor binding, or Smad2 phosphorylation. Levels of inhibitory Smad7 were also similar between FASC and control AECs (Supplemental Figure 5), indicating that α3 integrin regulation of EMT is distinct from a recently described mechanism in which α3 integrin regulates levels of Smad7 and pSmad2 in keratinocytes (28).

We recently observed that an immortalized α3 integrin–null kidney epithelial cell line also had defective responses to TGF-β1 compared with WT cells (29). Levels of pSmad2 following TGF-β1 stimulation were similar between a3 integrin–null and WT kidney epithelial cells. Smad7 levels were also independent of the presence or absence of α3 integrin in these kidney epithelial cells. The α3β1 integrin was also found to physically associate with TGF-β1 receptors as well as E-cadherin in a tripartite complex and to be required for TGF-β1–induced phosphorylation of β-catenin at Y654. Phosphorylation of Y654–β-catenin has previously been reported to be important for both its release from E-cadherin and stabilization from proteosomal turnover (30). We found that pY654–β-catenin formed a complex with pSmad2 shortly after TGF-β1 stimulation and was required for development of EMT
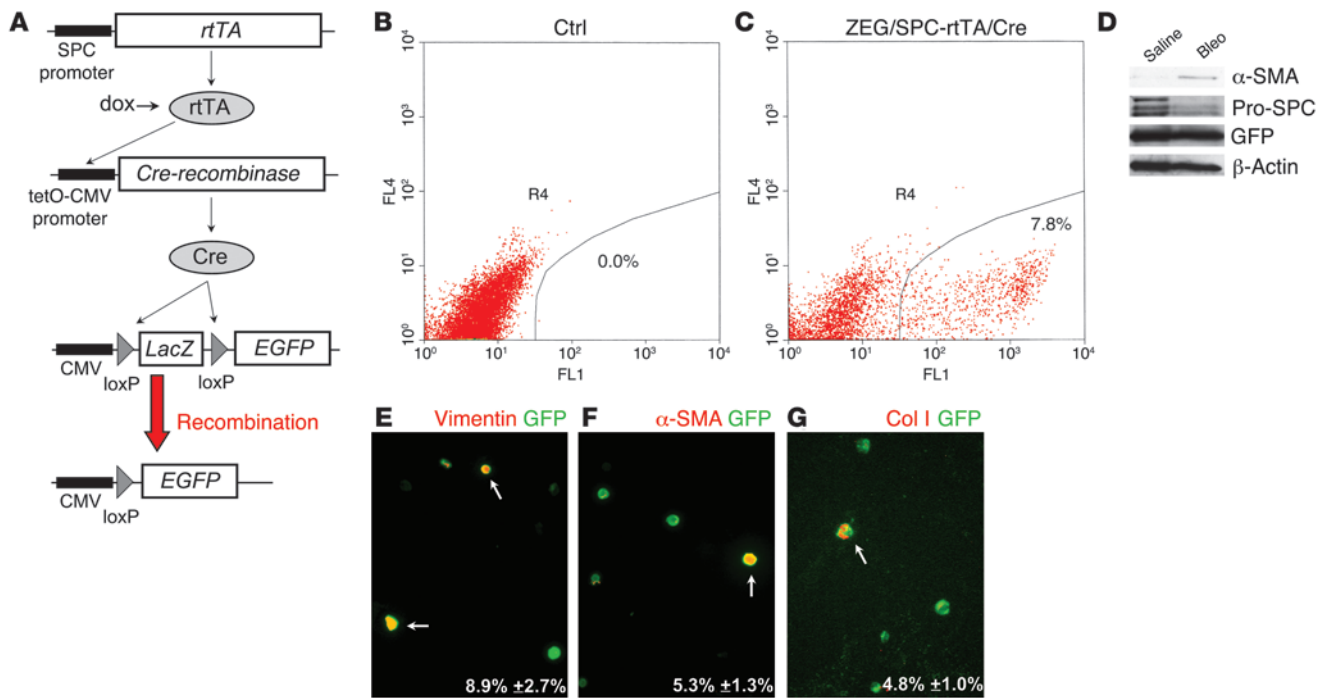
Figure 5
EMT develops in vivo following intratracheal injection of bleomycin. (**A**) In triple transgenic mice, rtTA is expressed in lung epithelial cells using the human SPC promoter. In the presence of doxycycline (dox), rtTA is an active transcriptional factor leading to expression of Cre recombinase and the removal of the floxed portion of the ZEG allele, resulting in lung epithelial cell–specific expression of GFP. (**B** and **C**) Density plots obtained during cell sorting for GFP-positive cells from whole lung single-cell suspensions prepared from littermate control (**B**) and triple transgenic (**C**; ZEG/SPC-rtTA/Cre) mice 17 days after intratracheal bleomycin injury. Percentages of GFP-positive cells are indicated. (**D**) Seventeen days after intratracheal saline or bleomycin injection, GFP-positive cells were sorted from whole lung single-cell suspensions of *ZEG/SPC-rtTA/tetO-Cre* mice. Immunoblot demonstrates de novo expression of α-SMA and downregulation of pro-SPC in epithelium-derived cells of bleomycin-injured mice. (**E**–**G**) Seventeen days after intratracheal saline or bleomycin injury, GFP-positive cells were sorted as described above and immunostained for GFP and mesenchymal markers vimentin (**E**), α-SMA (**F**), and procollagen I (**G**) and demonstrated expression of mesenchymal markers in epithelium-derived cells in bleomycin-injured mice, but none in saline-treated mice. The percentages of GFP-positive cells staining for mesenchymal markers are indicated. Original magnification, ×60.

in this kidney epithelial cell line (29). We therefore asked whether α3 integrin has a similar role in primary AECs and, if so, whether this mechanism operates in vivo.

As expected, immunoprecipitation of E-cadherin robustly coprecipitated α3 integrin in WT primary AECs (data not shown). To confirm that α3 integrin associates with TGF-β1 receptors, we used lentiviral-mediated transduction to express a myc-tagged TGF-β receptor I (mycRI). Lentiviral infections led to equal expression of mycRI in control and FASC AECs. Immunoprecipitation of mycRI led to coprecipitation of both α3 integrin and E-cadherin, consistent with the formation of a tripartite receptor complex (Figure 7). Interestingly, in FASC AECs, E-cadherin still associated with mycRI, indicating that the integrin is not required for this interaction. Specificity of these immunoprecipitations was confirmed by lack of precipitation of these proteins in cells infected with a control lentivirus expressing only GFP. These findings confirm the physical associations of α3 integrin, E-cadherin, and the TGF-β1 receptor in primary AECs and raise the possibility that α3 integrin in these cells could also regulate assembly of β-catenin/pSmad2 complexes, as we recently observed in a kidney cell line.

Primary AECs from FASC and littermate control mice were isolated, plated onto Fn for 48 hours to allow for activation of endog-

enous TGF-β1, and further stimulated with exogenous TGF-β1 for 1 hour. Control AECs demonstrated formation of β-catenin/ pSmad2 complexes by coimmunoprecipitation, while FASC AECs lacking α3 integrin failed to form this complex. Further, only WT AECs developed Y654 phosphorylation of β-catenin in response to TGF-β1 (Figure 7). Indeed, coimmunoprecipitation between pY654– β-catenin and pSmad2 was as robust as the total β-catenin/pSmad2 coimmunoprecipitation, indicating that pY654–β-catenin is likely the principal form of β-catenin in complex with pSmad2. Thus the α3 integrin is critical to formation of pY654–β-catenin/pSmad2 complexes in AECs. Finally, primary WT AECs cultured on Fn for 4 days demonstrated nuclear accumulation of pY654–β-catenin by immunostaining (Figure 7F). Many pY654–β-catenin–positive cells had also formed α-SMA stress fibers consistent with EMT.

pY654–β-catenin/pSmad2 complexes in mouse and human lung tissues. To extend this analysis in vivo, we performed coimmunoprecipitation on fresh whole lung lysates from FASC mice and littermate controls treated with saline and bleomycin (Figure 8A). WT mice demonstrated increased levels of pSmad2 2 weeks after bleomycin injury compared with saline-treated WT mice, consistent with activation of TGF-β1 signaling during fibrogenesis. FASC mice treated with bleomycin also demonstrated levels of pSmad2 sim-
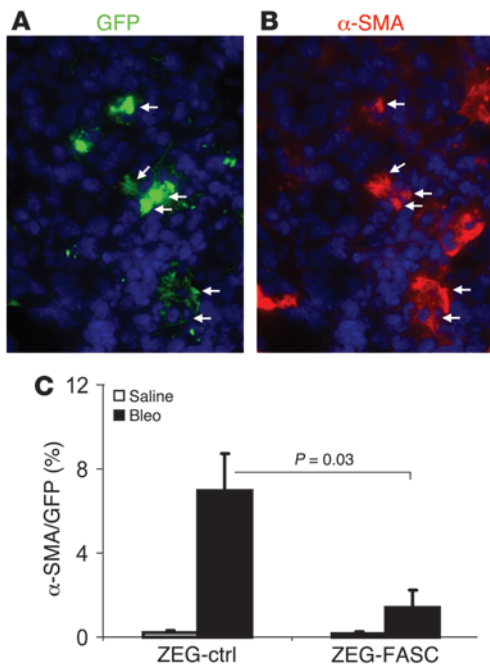
Figure 6

Lung epithelial cell α3 integrin regulates EMT in vivo. (**A** and **B**) Lung sections (original magnification, ×60) from a triple transgenic *ZEG/SPC-rtTA/tetO-Cre/α3^{WT/WT}* mouse 17 days after intratracheal bleomycin injury, immunostained for GFP (**A**) and α-SMA (**B**). Multiple cells costaining GFP and α-SMA are indicated by arrows. (**C**) Percentage of GFP-positive cells co-expressing α-SMA in ZEG-FASC (*ZEG/α3^{fl/fl}/SPC-rtTA/tetO-Cre*) and littermate control (*ZEG/α3^{fl/WT}* or *α3^{WT/WT}/SPC-rtTA/tetO-Cre*) mice treated with saline or bleomycin injection. Control mice demonstrated a marked increase in cells co-expressing α-SMA and GFP after bleomycin injury compared with FASC mice (*n* = 4 per group).

within and around clusters of myofibroblasts in α3^{+/+} control mice (mice that have normal levels of α3 integrin) injured with bleomycin but not in FASC mice. Although α3 integrin is deficient only in lung epithelial cells in the FASC mouse, this selective deficiency virtually completely abrogates formation of β-catenin/pSmad2 complexes in the whole lung in this model, implying that these transcriptional complexes are largely initiated in epithelial cells in response to TGF-β1.

To assess whether β-catenin/pSmad2 complexes accumulate in IPF, we used flash-frozen lung tissue obtained by biopsy at the time of diagnosis from 5 patients with IPF and compared them with flash-frozen normal human lung tissues and lung tissues from 6 patients with emphysema, a common lung disease associated with subepithelial fibrosis. Tissues were lysed and analyzed by immunoblot and immunoprecipitation. In general, levels of pSmad2 were consistently higher in IPF (samples F1–F5) than normal lung lysates (samples N1–N4) (Figure 9A). One of the nonfibrotic lung samples (N1) demonstrated high levels of pSmad2 by

ilar to WT mice treated with bleomycin. Of note, saline-treated (and completely uninjured) FASC mice demonstrated relatively high levels of baseline pSmad2. However, despite similar levels of pSmad2 after bleomycin injury, immunoprecipitation of β-catenin only coprecipitated pSmad2 in WT whole lung lysates but not in FASC whole lung lysates, confirming an α3 integrin–dependent β-catenin/pSmad2 complex formation in vivo during fibrogenesis. Fresh frozen lungs from FASC and littermate control mice 17 days after bleomycin injury were sectioned and immunostained for pY654–β-catenin and α-SMA (Figure 8, B and C). Nuclear pY654–β-catenin staining was seen

Figure 7

α3 integrin regulates association between β-catenin and pSmad2 ex vivo. (**A** and **B**) Primary AECs from FASC (**B**) and littermate control (**A**) mice were cultured on Fn for 4 days, then stained for F-actin with phalloidin and counterstained with DAPI (original magnification, ×60). Control cells demonstrated actin stress fibers consistent with a mesenchymal morphology, while FASC AECs demonstrated cortical actin staining consistent with an epithelial morphology. (**C**) Primary AECs from FASC or littermate control mice lacking 1 of the 3 transgenes were analyzed by immunoblot immediately after isolation (day 0) and 4 days after culturing on Fn-coated surfaces (day 4). FASC AECs had a blunted expression of mesenchymal markers collagen I, α-SMA, and vimentin. (**D**) Primary AECs were infected with lentivirus expressing mycRI or GFP as a control. Immunoprecipitation of mycRI demonstrated coprecipitation of α3 integrin and E-cadherin. (**E**) Coimmunoprecipitation of β-catenin (β-cat) and pSmad2 was seen with AECs from α3^{+/+} (control) but not AECs from FASC mice plated on Fn for 4 days to allow activation of TGF-β1 (top blot). TGF-β1–dependent tyrosine phosphorylation of β-catenin at Y654 and pY654–β-catenin/pSmad2 coprecipitation was only seen with AECs from α3^{+/+} mice (bottom blot). (**F**) Primary AECs cultured on Fn for 4 days then stained for α-SMA and pY654–β-catenin showed nuclear accumulation of β-catenin (original magnification, ×40).
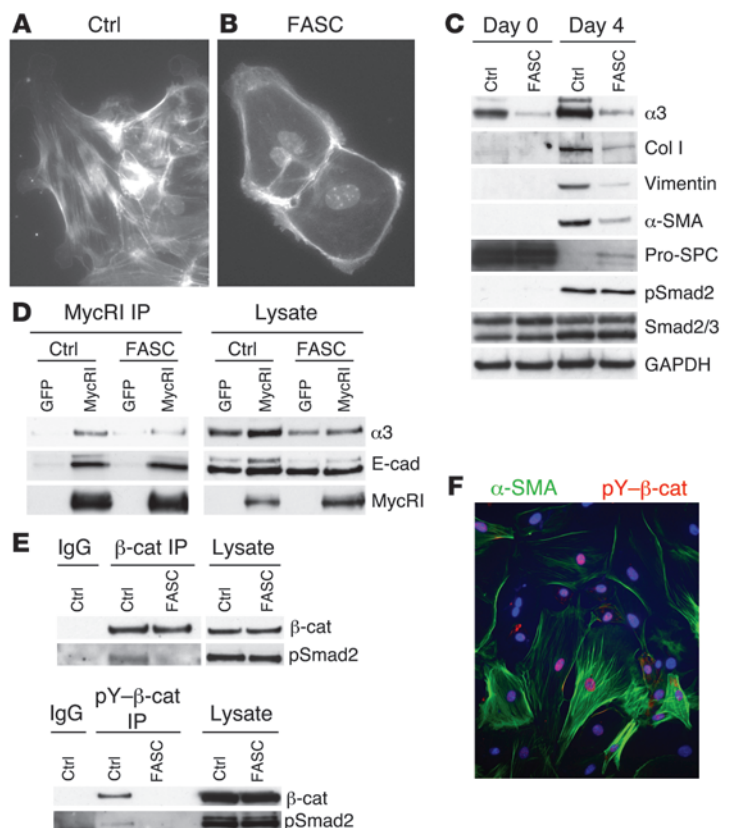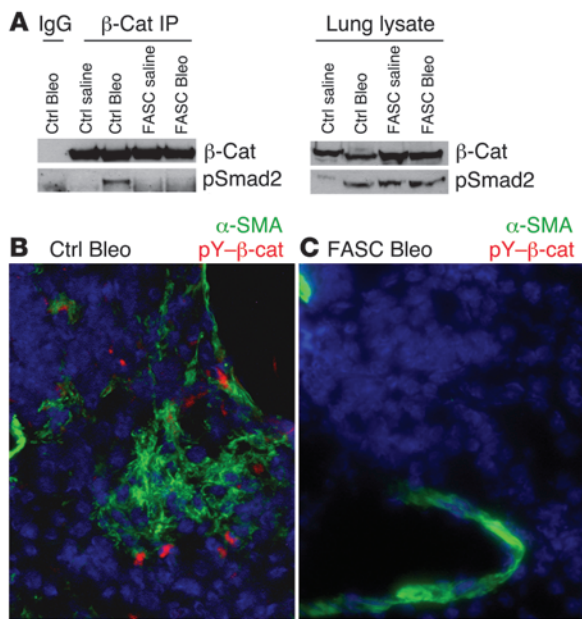
Figure 8
β-catenin and pSmad2 coimmunoprecipitation in murine lungs following bleomycin injury. (**A**) Two weeks after intratracheal bleomycin or saline injection, FASC and littermate control lungs were lysed and analyzed by immunoblot and immunoprecipitation for β-catenin. Control mice injured with bleomycin demonstrated β-catenin/pSmad2 coimmunoprecipitation. (**B** and **C**) FASC (**C**) and littermate control (**B**) fresh frozen lung section (original magnification, ×60) 17 days after bleomycin injury immunostained for α-SMA (green) and pY–β-catenin (red). Numerous nuclei stained for pY–β-catenin within and around myofibroblast clusters in littermate control but not FASC mice.

Discussion
The findings reported here add insight into the pathobiology of tissue fibrosis and demonstrate what we believe is a novel role for α3β1 integrin. EMT has been demonstrated in vivo in several animal models of fibrosis (8, 25, 26), but the contribution of this transition for the fibrotic outcome has remained uncertain. In part, this is because secreted factors that induce or inhibit EMT are also important regulators of fibroblast function. Generation of mice with lung epithelial cell–specific loss of α3 integrin indicates that this laminin receptor has no essential function in maintaining normal airway barrier integrity. Instead, α3 integrin is revealed to be a critical regulator of EMT and tissue remodeling in response to injury. In a well-described model of lung injury and fibrosis, lung injury and inflammation were intact and possibly exaggerated in α3 integrin–deficient mice, but the degree of in vivo EMT and fibrosis were dramatically attenuated. To our knowledge, this is the first report of attenuating fibrosis by epithelial cell–specific deletion of a protein involved in regulating EMT. Thus, these data provide the strongest evidence yet that EMT not only occurs dur-

immunoblot. Levels of β-catenin were comparable among the samples. Immunoprecipitation for β-catenin led to robust coprecipitation of pSmad2 in all IPF samples but in none of the normal lung samples. Interestingly, the 1 nonfibrotic lung sample (N1) that demonstrated elevated levels of pSmad2 within the lung lysate did not show β-catenin/pSmad2 coimmunoprecipitation, suggesting that this association is specific to fibrotic lung disease. Furthermore, immunoprecipitation for pY654–β-catenin demonstrated β-catenin tyrosine phosphorylation only in IPF lung tissues and not in normal lung (Figure 9A) or in emphysema lung tissue (Supplemental Figure 6). Accordingly, pSmad2 coimmunoprecipitated with pY654–β-catenin in IPF samples but not in either normal or emphysema lung samples. Thus, tyrosine phosphorylation of β-catenin at Y654 and its association with pSmad2 are prominent in IPF, but seemingly absent in normal or emphysematous lungs.
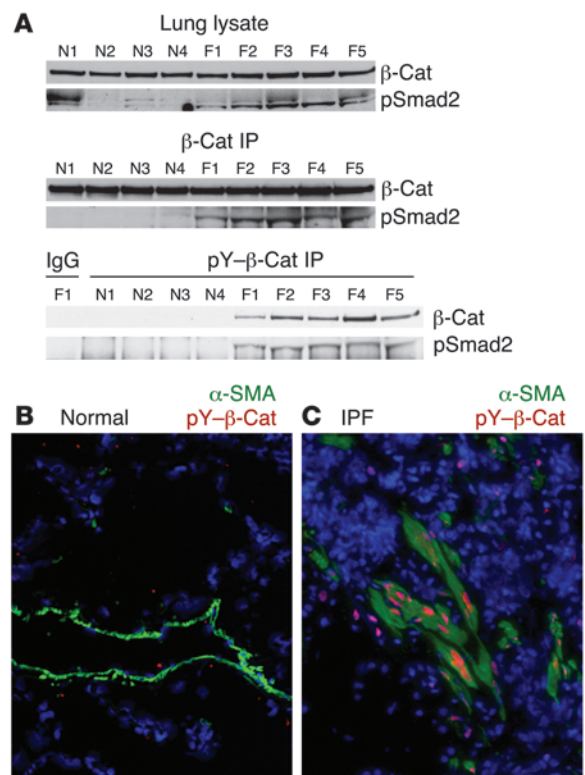
Finally, we explored where in IPF lungs the pY654–β-catenin accumulated. Flash-frozen normal or IPF lung tissues were also immunostained for pY654–β-catenin and α-SMA. Again, distinct nuclear pY654–β-catenin staining was observed within a significant fraction of nuclei of IPF but not normal lungs. Most of the staining was strikingly localized to subepithelial myofibroblasts, and most such myofibroblasts displayed nuclear pY654–β-catenin accumulation (Figure 9, B and C). In addition, a small number of AECs in IPF lung showed nuclear accumulation of pY654–β-catenin.

Figure 9
pY654–β-catenin/pSmad2 complexes in IPF lungs. (**A**) Normal human lung samples (N1–N4) and IPF lung samples (F1–F5) were lysed and analyzed by immunoblot and immunoprecipitation for β-catenin or pY654–β-catenin. All IPF samples demonstrated increased pSmad2 and pY–β-catenin. β-catenin and pY–β-catenin coimmunoprecipitated with pSmad2 in IPF samples, but not normal lung samples. (**B** and **C**) Fresh frozen normal (**B**) and IPF (**C**) lung sections (original magnification, ×20) were stained for pY–β-catenin (red) and α-SMA (green). Numerous nuclei stained for pY–β-catenin in IPF lung but not in normal lung. Myofibroblasts in IPF lung were frequently pY–β-catenin positive.

ing injury-induced fibrogenesis but is important to the outcome. In addition, findings reported here implicate a surprising mechanism by which the integrin regulates EMT. Rather than classic matrix-dependent signaling through integrin clustering, we postulate that the capacity of α3β1 integrin to engage laminin and E-cadherin may mainly be a sensing function that regulates epithelial responses to TGF-β1. In this scenario, engagement of the α3 integrin on the laminin-rich basement membrane or in cell-cell contact suppresses its role in promoting TGF-β1–induced EMT. This model clarifies our previous observations that AECs cultured on laminin/collagen IV form tight cell-cell borders and are resistant to EMT even when stimulated with exogenous TGF-β1 (8). Cells cultured on Fn, which is not an α3β1 integrin ligand, undergo TGF-β1–mediated EMT. In concurrent parallel studies of an α3 integrin–deficient kidney cell line reconstituted with WT α3 integrin or an α3 integrin mutant unable to bind laminin-5, we observed engagement of laminin-5 to suppress TGF-β1–dependent Y654–β-catenin phosphorylation, β-catenin/pSmad2 complexes, and mesenchymal gene expression. In this context, the protection of FASC mice from EMT may have resulted in part from the increased type IV collagen observed in the lungs of these mice (Figure 2). Type IV collagen has been reported to be a ligand for α3β1 integrin (31), and kidney epithelial cells cultured on type IV collagen are reportedly resistant to EMT (32). Further studies into the mechanism of type IV collagen accumulation in FASC mice and the role of collagen IV in EMT and lung fibrosis are ongoing.

Synergistic interactions on gene transcription between effectors of the TGF-β1 and Wnt signaling pathways, Smads and β-catenin respectively, have been previously reported (33). Although Smads and β-catenin (34) are each well-described transcriptional effectors of EMT, coordination between these pathways during EMT has not been defined. α3β1 integrin is identified here as a critical nidus at which these prominent EMT pathways converge. But rather than acting through Wnt-dependent inhibition of serine phosphorylation of β-catenin, in the presence of active TGF-β1, α3β1 integrin empowers tyrosine phosphorylation of β-catenin at Y654 and formation of pY–β-catenin/pSmad2 transcriptional complexes, promoting EMT. Several lines of evidence favor the conclusion that formation of these complexes is important to fibrogenesis. (a) pY654–β-catenin/pSmad2 complexes only form under conditions supporting EMT and fibrosis. Clearly, pSmad2 generation per se is not sufficient for either EMT or lung fibrosis. Indeed, recent studies of conditionally deleted Smad2 in liver and skin imply that Smad2 alone may suppress EMT (35, 36). Thus, the function of pY654–β-catenin is unlikely to be to simply augment pSmad2 signaling, but rather to redirect or possibly even to inhibit pSmad2 signaling. Epithelial-specific deficiency of α3 integrin led to loss of pY654–β-catenin phosphorylation both ex vivo in primary AECs and in vivo in the bleomycin-injured whole lung. Loss of pY654–β-catenin mirrored attenuation of EMT and fibrosis. (b) In kidney epithelial cells exposed to active TGF-β1, stable expression of a dominant-negative β-catenin blocked α-SMA responses even though no evidence of β-catenin/Lef1 signaling was detectable, consistent with prior studies indicating that TGF-β1 does not directly activate catenin/Lef1 signaling (37). (c) Immunostaining of lung tissues obtained from IPF patients revealed that nuclear pY654–β-catenin was largely confined to α-SMA–positive fibroblasts and a subset of AECs. No staining was observed in normal or emphysematous lungs (Figure 9 and Supplemental Figure 6). Interestingly, the pattern of nuclear

accumulation of pY654–β-catenin was different in injured murine lungs (Figure 8). A smaller fraction of myofibroblasts exhibited nuclear staining, possibly consistent with the less well-developed myofibroblast phenotype and limited nature of the injury in the bleomycin model as compared with IPF. Although it remains to be defined exactly how pY654–β-catenin acts along with pSmad2 to promote myofibroblast formation, and whether persistent nuclear accumulation further drives the process, we speculate that the appearance of nuclear pY654–β-catenin may be a novel diagnostic biomarker of in vivo EMT during tissue remodeling.

Although myofibroblast accumulation and fibrosis in injured murine lungs closely parallels EMT, we cannot exclude the possibility that epithelial cells contribute to pulmonary fibrosis by additional α3 integrin–dependent mechanisms. For example, the 2-fold increase in type II AECs and alveolar macrophage numbers (Figures 3 and 4) could reflect additional unmeasured alterations in α3 integrin–null AEC function that act concurrently to attenuate fibrogenesis. Indeed it is unlikely that most or all myofibroblasts arise from EMT during lung tissue remodeling, though myofibroblast accumulation is markedly diminished with only epithelial cell loss of α3 integrin. In the presence of α3 integrin–deficient AECs, fibroblasts (or myofibroblasts) potentially originating from other cell types were not able to compensate during bleomycin-induced fibrosis. It is also possible that epithelial cells reprogrammed in the lung during EMT may be important in initiating fibrogenesis by driving resident fibroblast proliferation and activation. If so, the contribution of EMT to fibrogenesis may be greater than a simple reflection of the fraction of fibroblasts that are EMT-derived. Fibroblasts from different origins may harbor unique features rather than blending into a homogeneous pool of cells. In support of this idea is a recent report indicating fibroblast strains derived from IPF patients and maintained in culture had distinct expression profiles, including markers indicative of epithelial origin (38). The ability to permanently delete intracellular signaling proteins specifically within lung epithelial cells offers the potential to further define the intricate interconnections between epithelial and mesenchymal cells important to fibrogenesis.

Finally, our findings may have therapeutic implications. Although multiple studies have demonstrated the importance of TGF-β1 to tissue fibrogenesis, a major limitation to the use of non-specific blocking agents of TGF-β1 signaling as antifibrotic therapy is the expected toxicity of such inhibition in multiple organs, especially the likelihood of autoimmunity (39). Dissecting the fibrogenic aspects of TGF-β1 signaling from other TGF-β1 responses is therefore an important next step in potential therapy. The distinct pathway of the α3β1 integrin–dependent, TGF-β1–initiated β-catenin/pSmad2 interaction described here must be active in IPF lung because we are able to demonstrate dramatic accumulation of nuclear pY654–β-catenin in IPF lung. This interaction is absent in normal lung, even when there is evidence for TGF-β1 activation, and it is absent in at least one other disease state, emphysema. Targeting physical determinants of E-cadherin/TGF-β1 receptor association, β-catenin tyrosine phosphorylation, or pY654–β-catenin/pSmad2 complex formation may offer therapeutic potential for attenuation of interstitial fibrosis without broadly interrupting the many physiological effects of TGF-β1.

Methods

Patient tissue sample accrual and processing. Written informed consent was obtained from all subjects, and the study was approved by the UCSF Com-

mittee on Human Research. IPF lung tissues were obtained from diagnostic lung biopsy or explanted lung during lung transplantation. IPF patients underwent a history, physical examination, high-resolution computed tomography, pulmonary function testing, and diagnostic lung biopsy. In all cases the pathologic diagnosis was usual interstitial pneumonia (UIP) and the consensus clinical diagnosis was IPF. Emphysema tissues were obtained from explanted lung during lung transplantation. In all cases the pathologic and clinical diagnosis was emphysema. Normal human lung tissue was obtained from human lungs not used by the Northern California Transplant Donor Network. Previous studies indicate that these lungs are physiologically and pathologically normal (40). Lung tissue was either directly snap-frozen in liquid nitrogen or inflated with PBS and embedded in OCT prior to snap-freezing. Samples were stored at –80°C until use for experiments. For immunoblot and immunoprecipitation experiments, frozen lung tissue was pulverized in a stainless steel tissue pulverizer (Fisher Scientific) pre-cooled in liquid nitrogen. Pulverized frozen lung tissue was immediately lysed and analyzed as described below.

Reagents. pSmad2 antibody was purchased from Calbiochem. Polyclonal pro-SPC antibody and plasma Fn were purchased from Chemicon. Monoclonal E-cadherin antibody was from Zymed. Matrigel, collagen I, and antibodies to E-cadherin, β-catenin, and α3 integrin were from BD Biosciences — Transduction Laboratories. Polyclonal myc antibody, α-SMA, vimentin, and β-actin antibodies were from Sigma-Aldrich. Polyclonal β-catenin antibody was from Cell Signaling. Collagen I, FITC-conjugated GFP, and GAPDH antibodies were from Abcam. Smad2/3, Smad7, laminin-5 (γ2), and secondary HRP-conjugated antibodies were from Santa Cruz Biotechnology Inc. Ki67 antibody was from Dako. Polyclonal GFP antibody, pY654–β-catenin, rhodamine-conjugated phalloidin, and FITC- and PE-labeled secondary antibodies were purchased from Invitrogen. Purified human KGF was purchased from PeproTech, and purified human TGF-β1 was purchased from R&D Systems. Small airway basal media and small airway growth media were purchased from Lonzo. Polyclonal collagen IV (α3) antibody was a gift from Raghu Kalluri (Harvard University, Cambridge, Massachusetts, USA).

Plasmid constructs and virus production. mycRI was a gift from Yoav Henis (41) (Tel Aviv University, Tel Aviv, Israel) and the Margaret Wheelock and Keith Johnson laboratory (University of Nebraska Medical Center, Omaha, Nebraska, USA) and was cloned into a modified version of pSicoR-GFP enabling lentiviral-mediated expression. pSicoR-GFP (42) was provided by Michael McManus and was modified by Jonathon Alexander and Chi-Hui Tang (all from UCSF). Lentivirus was produced by the UCSF Lentiviral Core Facility. Primary AECs were infected with 2 rounds of lentivirus encoding GFP or mycRI (10 pfu/cell) in the presence of polybrene (6 μg/ml) on days 1 and 2 after seeding.

Genetically modified mice. To generate conditional α3 integrin–null mice, a targeting vector was construction using the pDELBOY vector (43), such that LoxP sites flanked exon 3 of the α3 integrin gene and Frt sites flanked a NeoR cassette downstream of exon 2. After homologous recombination in embryonic stem cells and derivation of mice containing this allele, the Frt NeoR Frt cassette was removed by mating these mice with mice expressing FlpE in the germ line (a gift from Susan Dymecki, Harvard University, Boston, Massachusetts, USA). This left a single Frt site between exon 2 and the LoxP site upstream of exon 3. The loxP sites flanking exon 3 subject this portion of the floxed α3 integrin gene to removal by cre, resulting in early translational termination in exon 4 (Figure 1A). The resulting conditional α3 integrin–null mice were maintained with a C57BL6/129 background. PCR was used for genotyping of the floxed α3 integrin allele using primers 5′-TGATGACTATACCAACCGGAC-3′ (forward) and 5′-ACTCCAAGCCA-CATATCCTC-3′ (reverse), such that the floxed α3 integrin allele yielded an approximately 620-bp fragment and the WT allele yielded an approximately 540-bp fragment.

Triple transgenic mice with lung epithelial cell–specific loss of α3 integrin were obtained by breeding and termed *FASC* mice. In experiments using FASC mice or cells from FASC mice, littermate controls lacking at least 1 of the 3 transgenes were used. Conditional ZEG mice, in which GFP is expressed after cre-mediated recombination, have been previously described (27). Triple transgenic *ZEG/SPC-rtTA/tetO-Cre* mice or quadruple transgenic mice also homozygous for the floxed α3 integrin transgene were obtained by breeding, resulting in GFP expression in lung epithelial cells and their derivatives. Pregnant females were maintained on doxycycline throughout gestation, and resulting litters were genotyped as previously described (8, 27). All mice were bred and maintained in a specific pathogen–free environment. Mouse lung sections (5–7 μm thick) were stained by H&E and trichrome by the UCSF Research Morphology Core Facility.

Recombination of floxed α3 integrin by PCR. Recombination of the floxed α3 integrin allele was determined by PCR using primers that encompass the approximately 2.5-kb floxed region: 5′-TGATGACTATACCAACCGGAC-3′ (forward) and 5′-CAGAAGGCATGAATTTGAGAG-3′ (reverse), such that the recombined floxed α3 integrin produced a 1-kb band while the non-recombined floxed α3 integrin produced a 3.5-kb band. DNA from murine embryonic fibroblasts (MEF cells) isolated from floxed α3 integrin mice and treated in vitro with adenovirus encoding cre (a gift from Lilly Wu, UCLA, Los Angeles, California, USA) was used as a positive control for the recombined floxed α3 integrin band.

Mouse type II AEC isolation and culture. Isolation of primary AECs was performed as previously described (8) following the method of Corti (44) with minor modifications. Typical yields were about 10^6 cells per mouse, which were more than 95% type II AECs as assessed by cytospin and immunostaining for pro-SPC. Cells were either analyzed immediately after isolation or cultured on Fn-coated plates in SAGM supplemented with 5% CT-FBS and KGF (10 ng/ml) in a 37°C, 5% CO_2 incubator as previously described (8). Whole lung single-cell suspension was obtained from murine lungs as previously described (8), then immediately FACS sorted for GFP-expressing cells for further analysis.

Bleomycin lung injury and measurement of fibrosis. Six-week-old FASC mice or littermate controls were endotracheally instilled with saline or 1.3 U/kg of bleomycin (Blenoxane; Bristol-Myers Squibb) dissolved in saline via surgical tracheotomy (45). Mice were sacrificed 5–21 days after injury. Hydroxyproline was measured by methods previously described (45). Briefly, homogenates from the entire left lungs were incubated on ice in trichloroacetic acid, then baked in 12N HCl. Aliquots of the samples reconstituted in distilled water were added to 1.4% chloramine T in 10% isopropanol and 0.5 M sodium acetate for 20 min. Erlich's solution was added, and the samples were incubated at 65°C for 15 minutes. Absorbance at 550 nm was measured. Type I and type IV collagen was measured by immunoblot by methods previously described (46, 47).

Measurement of lung permeability and compliance. Lung permeability was determined by extravasation of intravascular ^{125}I-labeled albumin into the lungs as previously described (48) and expressed as extravascular plasma equivalent normalized to plasma volume (EVP%). Total protein concentration (mg/ml) from bronchoalveolar lavage (BAL) 5 days after intratracheal saline or bleomycin injury was measured using the BCA assay (Pierce Biotechnology) per the manufacturer's protocol. Lung compliance (μl/cm H_2O) was determined from anesthetized and paralyzed ventilated mice as previously described (48). Excess lung water was determined as previously described (48). For each experiment, n = 4–6 mice per group.

Immunofluorescence microscopy. Isolated cells and 5- to 7-μm cryosections were stained by immunofluorescence as previously described (8). For immunostaining mouse lung with mouse monoclonal anti–pY654–β-catenin, the antibody was directly conjugated using Alexa Fluor Microscale Protein Labeling Kit (Invitrogen) per the manufacturer's

instructions. Stained sections were visualized on a Nikon fluorescent microscope and images captured with a SPOT 2.3.1 camera (Diagnostic Instruments) and analyzed using SPOT 4.0.9 software (Diagnostic Instruments). For cellular quantification of myofibroblasts from immunostained slides, at least 10 fields (×20) from each mouse were visualized and quantified independently by 2 investigators in a blinded fashion. SimplePCI (Hamamatsu Corp.) was used for all other cellular quantification of immunostained slides.

Statistics. Data are expressed as mean ± SEM. For evaluation of group differences, the 2-tailed Student's *t* test was used assuming equal variance. A *P* value of less than 0.05 was accepted as significant.

Flow cytometry. Cells were analyzed for expression of GFP by flow cytometry using FACSCalibur cytometer (BD Biosciences) and CellQuest Pro software or sorted for GFP-expressing cells using a MoFlo Cell Sorter (Dako) at the UCSF Flow Cytometry Core Facility.

Immunoblot. Tissue and cells were lysed in RIPA buffer (150 mM NaCl, 50 mM Tris, pH 8.0, 1% Triton X-100, 0.5% sodium deoxycholate, 0.1% SDS, supplemented with protease and phosphatase inhibitors) and analyzed by immunoblot as previously described (49). Scanned immunoblots are representative of at least 3 separate experiments. Densitometry was quantified using NIH ImageJ.

Ex vivo and in vivo immunoprecipitation. For primary AEC coimmunoprecipitation of mycRI and α3 integrin, cells were seeded onto Fn-coated plates. Cells were infected with lentivirus encoding GFP or mycRI on days 1 and 2 after seeding then lysed in Triton buffer on day 5. Equal concentrations of clarified lysates were incubated for 2 hours at 4°C with monoclonal myc antibody and were then precipitated with protein A and protein G agarose beads (Invitrogen) overnight at 4°C. Beads were washed and then analyzed by immunoblot for α3 integrin, E-cadherin, and mycRI. For primary AEC immunoprecipitation of β-catenin and pY–β-catenin, equal numbers of FASC or littermate control AECs were seeded on Fn-coated plates. Three days after seeding, cells were

rinsed twice with PBS supplemented with sodium orthovanadate and Phosphatase Inhibitor Cocktail 2 (Sigma-Aldrich) and then lysed in RIPA buffer. Clarified lysate was immunoprecipitated for β-catenin and pY–β-catenin using monoclonal antibodies as described above then analyzed by immunoblot for β-catenin and pSmad2. For in vivo immunoprecipitation from murine lungs, FASC and littermate control mice were sacrificed 2 weeks after intratracheal injection with saline or bleomycin. Lungs were perfused and lavaged with PBS supplemented with sodium orthovanadate and Phosphatase Inhibitor Cocktail 2 and then immediately lysed in RIPA buffer. Clarified lysates were further precleared by incubating with protein A and protein G beads. The precleared supernatants were then immunoprecipitated for β-catenin and pY–β-catenin as described above. For in vivo immunoprecipitation of human lung samples, snap-frozen lungs were pulverized and lysed in RIPA. Clarified lysates were further precleared with secondary anti-rabbit HRP antibody and protein A and protein G beads. The precleared supernatants were then immunoprecipitated for β-catenin and pY–β-catenin as described above.

1. Selman, M., King, T.E., and Pardo, A. 2001. Idiopathic pulmonary fibrosis: prevailing and evolving hypotheses about its pathogenesis and implications for therapy. *Ann. Intern. Med.* **134**:136–151.
2. Thannickal, V.J., Toews, G.B., White, E.S., Lynch, J.P., 3rd, and Martinez, F.J. 2004. Mechanisms of pulmonary fibrosis. *Annu. Rev. Med.* **55**:395–417.
3. Kalluri, R., and Neilson, E.G. 2003. Epithelial-mesenchymal transition and its implications for fibrosis. *J. Clin. Invest.* **112**:1776–1784.
4. Savagner, P. 2001. Leaving the neighborhood: molecular mechanisms involved during epithelial-mesenchymal transition. *Bioessays.* **23**:912–923.
5. Thiery, J.P. 2003. Epithelial-mesenchymal transitions in development and pathologies. *Curr. Opin. Cell Biol.* **15**:740–746.
6. Zeisberg, M., and Kalluri, R. 2004. The role of epithelial-to-mesenchymal transition in renal fibrosis. *J. Mol. Med.* **82**:175–181.
7. Thiery, J.P., and Sleeman, J.P. 2006. Complex networks orchestrate epithelial-mesenchymal transitions. *Nat. Rev. Mol. Cell Biol.* **7**:131–142.
8. Kim, K.K., et al. 2006. Alveolar epithelial cell mesenchymal transition develops in vivo during pulmonary fibrosis and is regulated by the extracellular matrix. *Proc. Natl. Acad. Sci. U. S. A.* **103**:13180–13185.
9. Bartram, U., and Speer, C.P. 2004. The role of transforming growth factor beta in lung development and disease. *Chest.* **125**:754–765.
10. Willis, B.C., et al. 2005. Induction of epithelial-mesenchymal transition in alveolar epithelial cells by transforming growth factor-beta1: potential role in idiopathic pulmonary fibrosis. *Am. J. Pathol.* **166**:1321–1332.
11. Zavadil, J., and Bottinger, E.P. 2005. TGF-beta and

epithelial-to-mesenchymal transitions. *Oncogene.* **24**:5764–5774.
12. Derynck, R., and Zhang, Y.E. 2003. Smad-dependent and Smad-independent pathways in TGF-beta family signalling. *Nature.* **425**:577–584.
13. Schmierer, B., and Hill, C.S. 2007. TGFbeta-SMAD signal transduction: molecular specificity and functional flexibility. *Nat. Rev. Mol. Cell Biol.* **8**:970–982.
14. Giancotti, F.G., and Ruoslahti, E. 1999. Integrin signaling. *Science.* **285**:1028–1032.
15. Hynes, R.O. 2002. Integrins: bidirectional, allosteric signaling machines. *Cell.* **110**:673–687.
16. Hollenbeck, S.T., et al. 2004. Type I collagen synergistically enhances PDGF-induced smooth muscle cell proliferation through pp60src-dependent crosstalk between the alpha2beta1 integrin and PDGFbeta receptor. *Biochem. Biophys. Res. Commun.* **325**:328–337.
17. Moro, L., et al. 1998. Integrins induce activation of EGF receptor: role in MAP kinase induction and adhesion-dependent cell survival. *EMBO J.* **17**:6622–6632.
18. Bhowmick, N.A., Zent, R., Ghiassi, M., McDonnell, M., and Moses, H.L. 2001. Integrin beta 1 signaling is necessary for transforming growth factor-beta activation of p38MAPK and epithelial plasticity. *J. Biol. Chem.* **276**:46707–46713.
19. Chattopadhyay, N., Wang, Z., Ashman, L.K., Brady-Kalnay, S.M., and Kreidberg, J.A. 2003. alpha3beta1 integrin-CD151, a component of the cadherin-catenin complex, regulates PTPmu expression and cell-cell adhesion. *J. Cell Biol.* **163**:1351–1362.
20. Chilosi, M., et al. 2003. Aberrant Wnt/beta-catenin pathway activation in idiopathic pulmonary fibrosis. *Am. J. Pathol.* **162**:1495–1502.

21. Kreidberg, J.A., et al. 1996. Alpha 3 beta 1 integrin has a crucial role in kidney and lung organogenesis. *Development.* **122**:3537–3547.
22. Madtes, D.K., et al. 1999. Transforming growth factor-alpha deficiency reduces pulmonary fibrosis in transgenic mice. *Am. J. Respir. Cell Mol. Biol.* **20**:924–934.
23. Zhao, J., et al. 2002. Smad3 deficiency attenuates bleomycin-induced pulmonary fibrosis in mice. *Am. J. Physiol. Lung Cell Mol. Physiol.* **285**:L585–L593.
24. Scotton, C.J., and Chambers, R.C. 2007. Molecular targets in pulmonary fibrosis: the myofibroblast in focus. *Chest.* **132**:1311–1321.
25. Iwano, M., et al. 2002. Evidence that fibroblasts derive from epithelium during tissue fibrosis. *J. Clin. Invest.* **110**:341–350.
26. Zeisberg, M., et al. 2007. Fibroblasts derive from hepatocytes in liver fibrosis via epithelial to mesenchymal transition. *J. Biol. Chem.* **282**:23337–23347.
27. Novak, A., Guo, C., Yang, W., Nagy, A., and Lobe, C.G. 2000. Z/EG, a double reporter mouse line that expresses enhanced green fluorescent protein upon Cre-mediated excision. *Genesis.* **28**:147–155.
28. Reynolds, L.E., et al. 2008. α3β1 integrin-controlled Smad7 regulates reepithelialization during wound healing in mice. *J. Clin. Invest.* **118**:965–974.
29. Kim, Y. et al. 2009. Integrin alpha3beta1-dependent beta-catenin phosphorylation links epithelial Smad signaling to cell contacts. *J. Cell Biol.* In press.
30. Piedra, J., et al. 2001. Regulation of beta-catenin structure and activity by tyrosine phosphorylation. *J. Biol. Chem.* **276**:20436–20443.
31. Borza, C.M., et al. 2006. Integrin alpha3beta1, a novel receptor for alpha3(IV) noncollagenous domain and a trans-dominant Inhibitor for inte-

grin alphavbeta3. *J. Biol. Chem.* **281**:20932–20939.

32. Zeisberg, M., et al. 2001. Renal fibrosis: collagen composition and assembly regulates epithelial-mesenchymal transdifferentiation. *Am. J. Pathol.* **159**:1313–1321.

33. Lei, S., Dubeykovskiy, A., Chakladar, A., Wojtukie-wicz, L., and Wang, T.C. 2004. The murine gastrin promoter is synergistically activated by transforming growth factor-beta/Smad and Wnt signaling pathways. *J. Biol. Chem.* **279**:42492–42502.

34. Yook, J.I., et al. 2006. A Wnt-Axin2-GSK3beta cascade regulates Snail1 activity in breast cancer cells. *Nat. Cell Biol.* **8**:1398–1406.

35. Hoot, K.E., et al. 2008. Keratinocyte-specific Smad2 ablation results in increased epithelial-mesenchymal transition during skin cancer formation and progression. *J. Clin. Invest.* **118**:2722–2732.

36. Ju, W., et al. 2006. Deletion of Smad2 in mouse liver reveals novel functions in hepatocyte growth and differentiation. *Mol. Cell. Biol.* **26**:654–667.

37. Lim, S.K., and Hoffmann, F.M. 2006. Smad4 cooperates with lymphoid enhancer-binding factor 1/

T cell-specific factor to increase c-myc expression in the absence of TGF-beta signaling. *Proc. Natl. Acad. Sci. U. S. A.* **103**:18580–18585.

38. Larsson, O., et al. 2008. Fibrotic myofibroblasts manifest genome-wide derangements of translational control. *PLoS ONE.* **3**:e3220.

39. Rubtsov, Y.P., and Rudensky, A.Y. 2007. TGFbeta signalling in control of T-cell-mediated self-reactivity. *Nat. Rev. Immunol.* **7**:443–453.

40. Ware, L.B., et al. 2002. Assessment of lungs rejected for transplantation and implications for donor selection. *Lancet.* **360**:619–620.

41. Gilboa, L., Wells, R.G., Lodish, H.F., and Henis, Y.I. 1998. Oligomeric structure of type I and type II transforming growth factor beta receptors: homo-dimers form in the ER and persist at the plasma membrane. *J. Cell Biol.* **140**:767–777.

42. Ventura, A., et al. 2004. Cre-lox-regulated conditional RNA interference from transgenes. *Proc. Natl. Acad. Sci. U. S. A.* **101**:10380–10385.

43. Rossi, D.J., et al. 2001. Inability to enter S phase and defective RNA polymerase II CTD phosphorylation

in mice lacking Mat1. *EMBO J.* **20**:2844–2856.

44. Corti, M., Brody, A.R., and Harrison, J.H. 1996. Isolation and primary culture of murine alveolar type II cells. *Am. J. Respir. Cell Mol. Biol.* **14**:309–315.

45. Munger, J.S., et al. 1999. The integrin alpha v beta 6 binds and activates latent TGF beta 1: a mechanism for regulating pulmonary inflammation and fibrosis. *Cell.* **96**:319–328.

46. Sugimoto, H., et al. 2006. Bone-marrow-derived stem cells repair basement membrane collagen defects and reverse genetic kidney disease. *Proc. Natl. Acad. Sci. U. S. A.* **103**:7321–7326.

47. Wang, X.M., et al. 2006. Caveolin-1: a critical regulator of lung fibrosis in idiopathic pulmonary fibrosis. *J. Exp. Med.* **203**:2895–2906.

48. Frank, J.A., Pittet, J.F., Wray, C., and Matthay, M.A. 2008. Protection from experimental ventilator-induced acute lung injury by IL-1 receptor blockade. *Thorax.* **63**:147–153.

49. Zhang, F., et al. 2003. Distinct ligand binding sites in integrin alpha3beta1 regulate matrix adhesion and cell-cell contact. *J. Cell Biol.* **163**:177–188.